Meteorological effects on PM$_{2.5}$ change over a receptor region in regional transport of air pollutants: observational study of recent year emission reduction in central China

Xiaoyun Sun[1], Tianliang Zhao[1], Yongqing Bai[2], Shaofei Kong[3], Huang Zheng[3], Weiyang Hu[1], Xiaodan

Ma[1], Jie Xiong[2]

[1]Collaborative Innovation Center on Forecast and Evaluation of Meteorological Disasters, Key Laboratory for Aerosol-Cloud-

Precipitation of China Meteorological Administration, PREMIC, Nanjing University of Information Science and Technology,

Nanjing, 210044, China

[2]Institute of Heavy Rain, China Meteorological Administration, Wuhan, 430205, China

[3]Department of Atmospheric Sciences, School of Environmental Studies, China University of Geosciences (Wuhan), Wuhan,

430074, China

Correspondence to: TianLiang Zhao (tlzhao@nuist.edu.cn)

Abstract. As an important issue in atmospheric environment, the contributions of anthropogenic emissions and meteorological

conditions to air pollution have been few assessed over the receptor region in regional transport of air pollutants. In this study

on observations of environment and meteorology over 2015-2019, the Kolmogorov–Zurbenko (KZ) filter was performed to

decompose the PM$_{2.5}$ variations into multi-time scale components over the Twain-Hu Basin (THB), a receptor region in

regional transport of air pollutants in central China, where the short-term, seasonal and long-term components accounted for

respectively 47.5%, 41.4% and 3.7% to daily PM$_{2.5}$ changes. The short-term and seasonal components dominated the day-to-

day PM$_{2.5}$ variations with long-term component determining the change trend of PM$_{2.5}$ concentrations over recent years. The

emission- and meteorology-related long-term PM$_{2.5}$ components over the THB were identified. The meteorological

contribution to PM$_{2.5}$ declining trend presented the distinct spatial pattern over the THB with northern positive rates up to

61.92% and southern negative rates down to -24.93%. The opposite effects of meteorology on PM$_{2.5}$ pollution could accelerate and offset the effects of emission reductions in the northern and southern THB, which is attributed to the upwind diffusion and

25   downward accumulation of air pollutants over the receptor region in regional PM$_{2.5}$ transport. It is noteworthy that the increasing conversion efficiencies of SO$_2$ and NO$_2$ to sulfate and nitrate for secondary PM$_{2.5}$ could offset the effects of PM$_{2.5}$ emission reduction on air pollution in the THB during recent years, revealing the enhancing contribution of gaseous precursor emissions to PM$_{2.5}$ concentrations with controlling anthropogenic emissions of PM$_{2.5}$ and the gaseous precursors over the receptor region in regional transport of air pollutants.

30

1. Introduction

Haze pollution with high levels of PM$_{2.5}$ (fine particulate matters with aerodynamic diameters equal to or less than 2.5 μm) has been a serious problem in atmospheric environment (Peng et al., 2016; Wang et al., 2016) with adverse influences on air quality and human health (Cao et al., 2012; Crouse et al., 2012). In recent years, the large areas over Central and Eastern

35   China (CEC) have undergone haze pollution with unprecedentedly high PM$_{2.5}$ levels in the regions covering North China Plain (NCP), Yangtze River Delta (YRD), Pearl River Delta (PRD) and Sichuan Basin (SB) (Zhang et al., 2012; Lin et al., 2018; Guo et al., 2017). In order to improve air quality with reducing air pollutant emissions, Chinese government has implemented an Action Plan of controlling anthropogenic emissions since September 2013 (http://www.gov.cn/xinwen/2018-02/01/content_5262720.htm, last access: August 21, 2021). Surface PM$_{2.5}$ concentrations exhibited 30%–40% decreases in

40   CEC over recent years (Xue et al., 2019; Zhang et al., 2019). However, the changes of air pollution are generally co-determined by air pollutant emissions and meteorological conditions. The contributions of changes in meteorology and anthropogenic emissions to the improvement of air quality need to be comprehensively investigated.

In addition to anthropogenic emissions of air pollutants, the meteorological conditions can alter the local accumulation, regional transport, chemical conversion, wet and dry depositions of air pollutants (Lu et al., 2017; Li et al., 2018). Severe haze

45   pollution always occurs in the wintertime under the stagnant meteorological conditions with weak near-surface wind, strong

temperature inversion, and high relative humidity in the atmospheric boundary layer, which are favorable for the accumulation

of air pollutants to form air pollution (Li et al., 2018; Miao et al., 2015; Tang et al., 2016). Meteorological conditions are

closely governed by synoptic circulations, modulating the atmospheric physical and chemical processes including regional

transport of air pollutants (Miao et al., 2017; Ning et al., 2019). The climate changes of East Asian monsoons largely influence

50 the seasonal and interannual variations of aerosol concentrations for air pollution over China (Zhu et al., 2012; Jeong and Park,

2017).

Assessments on contributions of anthropogenic emissions and meteorological changes to air quality improvement are an

important issue in environmental changes (Pearce et al., 2011; Zhang et al., 2018; Chen et al., 2019). The chemical transport

models have been widely used to quantify the meteorological effects on $PM_{2.5}$ variations by a linear additive relationship

55 between sensitivity and base simulations (Mueller and Mallard, 2011; Li et al., 2015b; Zhang et al., 2020). The contribution

of meteorological changes to $PM_{2.5}$ decreases was estimated at the averages of 10–20% with the interannual fluctuations of

about 5% in CEC from 2015 to 2019 through a model-based environmental meteorology index (Gong et al., 2021). The

accuracy of modeling assessments can be influenced by the uncertainties in emission inventories and the incomplete chemical

and physical mechanisms in air pollution simulation (Li et al., 2011). Based on statistical analysis on long-term observational

60 data, it was quantified that the emission control could explain more of the variances in $PM_{2.5}$ than meteorology (Gui et al.,

2019), and 12% of the observed $PM_{2.5}$ decrease was attributed to meteorological drivers in China since 2013 (Zhai et al., 2019).

However, the modeling and observational studies have mostly assessed the contribution of emissions and meteorology to

regional $PM_{2.5}$ variations in the source regions with high anthropogenic emissions of air pollutants, and there have been few

assessments on multi-scale changes of atmospheric environment over the receptor region in regional transport of air pollutants.

65 The Twain-Hu Basin (THB), featuring the lower lands (mainly less than 200 m in a. s. l.) of two provinces Hubei and

Hunan in central China (Fig. 1), is surrounded by the high air pollution regions NCP, YRD, PRD and SB. As such, it is the

receptor region in regional transport of air pollutants from the upstream region driven by East Asian monsoonal winds over

CEC (Shen et al., 2020). The heavy air pollution in the THB with a unique "non-stagnation" atmospheric boundary layer is

aggravated by regional PM$_{2.5}$ transport over CEC (Zhong et al., 2019; Yu et al., 2020). By cohesion with the heavy pollution

region of NCP through distinct transport channels, the regional transport from northern China to the THB contributed 70.5%

PM$_{2.5}$ concentrations to a wintertime heavy pollution episode in the THB (Hu et al., 2021). Thus, the contributions of air

pollutant emissions and meteorological conditions to air quality change over this air pollution region in central China need to

be specifically assessed with the long-term observations over recent years.

In this observational study, we investigated the multi-scale changes of PM$_{2.5}$ concentrations over the THB from 2015 to

2019 by establishing the statistic model with Kolmogorov–Zurbenko (KZ) filter, and then evaluated the contributions of

anthropogenic emissions and meteorological changes to the declining trends in PM$_{2.5}$ concentrations in this receptor region in

regional PM$_{2.5}$ transport over CEC during the past 5-year emission control. The analysis of THB's multi-scale air quality

changes can improve the understanding of the effects of emission mitigation and meteorological changes on environmental

change with regional transport of air pollutants.

2. Data and methods

2.1 Data

In order to analyze air quality changes in the THB, the observational data of hourly NO$_2$, SO$_2$ and PM$_{2.5}$ concentrations

from 2015 to 2019 were collected from the national air quality monitoring network (http://www.mee.gov.cn/, last access:

August 21, 2021). The air quality observation data are under quality control, based on China's national standard of air quality

observation.

The data of meteorological observations in the THB were sourced from the weather monitoring network of China

Meteorological Administration (http://data.cma.cn/, last access: August 21, 2021), including air temperature, relative humidity

(RH), sea level pressure (SLP), wind speed (WS) and precipitation with temporal resolutions of 3 h.

2.2 KZ filter

To better understand the multi-time scale variations of $PM_{2.5}$ and the relation to air pollutant emissions and meteorological

drivers, KZ filter (Rao and Zurbenko, 1994; Seo et al., 2018) is used to separate the daily data into multi-scale components,

based on an iterative moving average that removes high frequency variations in the data with the applications in study of air

95   pollutants, especially O_3 and $PM_{2.5}$ variations (Chen et al., 2019; Ma et al., 2016; Seo et al., 2014; Zheng et al., 2020).

The KZ filter $KZ_{m,p}$ with the length of moving average window m and the number of iterations p, can remove the high-

frequency component of period smaller than the effective filter width N ($\geq m \times p^{1/2}$). The KZ filter is applicable to the time

series with missing data owing to the iterative moving average process, which provides a high accuracy level to compare with

the wavelet transform method (Eskridge et al., 1997). In this study, we applied $KZ_{15,5}$ and $KZ_{365,3}$ filters to remove the

100   variations with the periods shorter than 33 days and 1.7 years.

A meteorological or environmental variable $X(t)$ observed in time series t can be decomposed into the short-term

component $X_{ST}(t)$ and the baseline component $X_{BL}(t)$ presenting as:

$$X(t) = X_{ST}(t) + X_{BL}(t). \tag{1}$$

The baseline component $X_{BL}(t)$ is obtained by applying the $KZ_{(15,5)}$ filter to $X(t)$, removing the short-term component

105    $X_{ST}(t)$ with the temporal period shorter than 33 days from the observed data, expressing with:

$$X_{BL}(t) = KZ_{(15,5)}[X(t)]. \tag{2}$$

The baseline component $X_{BL}(t)$ also can be separated into the daily climatic averages X_{BL}^{clm} over the study period

occupying most of the seasonality in $X_{BL}(t)$ and the residual $\varepsilon(t)$:

$$\varepsilon(t) = X_{BL}(t) - X_{BL}^{clm}. \tag{3}$$

110   To obtain the long-term component $X_{LT}(t)$ by removing the variations with the temporal period shorter than 1.7 years, the

$KZ_{365,3}$ filter is applied to $\varepsilon(t)$ expressed as follows:

$$X_{LT}(t) = KZ_{(365,3)}[\varepsilon(t)] \tag{4}$$

with the short-term component

$$X_{ST}(t) = X(t) - X_{BL}(t) \tag{5}$$

115   and the seasonal component

$$X_{SN}(t) = X_{BL}(t) - X_{LT}(t). \tag{6}$$

The KZ filter was used to separate the daily surface $PM_{2.5}$, NO_2 and SO_2 concentrations into short-term, seasonal and

long-term components in this study. The short-term component presents a synoptic-scale variation of meteorological influences,

which could control local accumulation and regional transport of air pollutants (Seo et al., 2017), partly associated with short-

120   term fluctuations in air pollutant emissions (Russell et al., 2010). The seasonal and long-term components are attributable to

the variations in air pollutant emissions related to human activities as well as the seasonal and interannual changes in

meteorological conditions (Kim et al., 2018).

2.3 Multiple linear regression of air pollutant changes with meteorological variables

125   By altering the local accumulation, regional transport, chemical conversion, wet and dry depositions of air pollutants, the

meteorological factors such as wind, RH, air temperature, air pressure and precipitation could exert significant impacts on

$PM_{2.5}$ changes (Sun et al., 2013; Li et al., 2018; Chen et al., 2020). Therefore, with the multiple factors of the baseline

components of 10-m WS, 2-m RH, 2-m air temperature, SLP and precipitation calculated by Eq. (2), a multiple linear

regression equation was stepwise established for the baseline component of $PM_{2.5}$ as follows:

130
$$PM_{2.5BL_{MLR}}(t) = a_0 + \sum_i a_i \, \mathrm{MET}_{BL_i}(t), \tag{7}$$

where $\mathrm{MET}_{BL_i}(t)$ ($i \in [1,5]$) is the baseline component of the meteorological variable i with $i=1,2,3,4,5$ respectively for

$WS_{BL}(t)$, $RH_{BL}(t)$, $T_{BL}(t)$, $SLP_{BL}(t)$, $Pre_{BL}(t)$. We fit the regression coefficient a_i for each meteorological variable and

the intercept a_0. The residual $\varepsilon_{PM_{2.5}}$ between $PM_{2.5BL}$ and $PM_{2.5BL_{MLR}}$ regressed with the multiple linear equation (7) is

given as:

135
$$\varepsilon_{PM_{2.5}}(t) = PM_{2.5BL}(t) - PM_{2.5BL_{MLR}}(t). \tag{8}$$

$\varepsilon_{PM_{2.5}}$ contains not only the variability of $PM_{2.5}$ related to long-term changes in air pollutant emissions but also the minor

seasonal change of $PM_{2.5}$ attributable to unconsidered meteorological influences in the multiple linear regression. By removing

the minor seasonal change from $\varepsilon_{PM_{2.5}}$ with the $KZ_{365,3}$ filter, the emission-related long-term component $PM_{2.5LT}^{emiss}(t)$

can be isolated as follows:

140
$$PM_{2.5LT}^{emiss}(t) = KZ_{(365,3)}[\varepsilon_{PM_{2.5}}(t)].\tag{9}$$

Here the long-term component of surface $PM_{2.5}$ concentration can be further separated into the emission- and meteorology-

related long-term components with Eqs. (9) and (4) (Seo et al., 2018). Similarly, the multi-time scale variations in SO_2 and

NO_2 with long-term variations related to changes in air pollutant emissions and meteorological drivers are decomposed by KZ

filter with multiple linear regression. Seo et al. (Seo et al., 2018) described the details of this method.

145

3. Results and discussion

3.1 Verification of PM₂.₅ decompositions in multi-scale variations

The daily $PM_{2.5}$ concentrations observed in 14 sites over the THB (Fig. 1) were decomposed into short-term, seasonal and

long-term components with Eqs. (4), (5) and (6) of the KZ filter. To verify the decomposition results, the spatial distribution

150   of total contributions of short-term, seasonal and long-term $PM_{2.5}$ components to the total variances of observed daily changes

in $PM_{2.5}$ concentrations over 2015–2019 were shown in Figure 2a. The total contribution of short-term, seasonal and long-term

components demonstrated the regional distribution with the high values exceeding 90% and the regional average of 92.7 % in

the THB (Fig. 2a), which presented a good decomposition of the multi-time scale components from the observed daily $PM_{2.5}$

with the KZ filter.

155   Based on the $PM_{2.5}$ decomposition results of KZ filter, the short-term, seasonal and long-term components respectively

accounted for 34.8%–53.8%, 29.2%–56.3% and 0.2%–9.8% of the total variances of daily $PM_{2.5}$ changes in the THB over

recent years (Figs. 2b, 2c and 2d), reflecting the different patterns of multi-time scale variations of $PM_{2.5}$ over this region in

central China with diverse effects of emissions and meteorology. The regional contributions of short-term, seasonal and long-

term components were averaged respectively with 47.5%, 41.4% and 3.7% to daily $PM_{2.5}$ changes over the THB (Fig. 2),

160   which could be reasonably verified that the daily variation in atmospheric pollutant was generally dominated by short-term

and seasonal components with long-term component determining the change trend (Ma et al., 2016; Yin et al., 2019a).

The short-term, seasonal and long-term $PM_{2.5}$ components were averaged in 14 sites of the THB to characterize the temporal variations of three components in the THB for 2015–2019 (Fig. 3). The observed daily $PM_{2.5}$ exhibited a distinct daily variation, with an overlapping of high frequency variations, which could be caused by mesoscale and synoptic scale

165   meteorological processes (Ma et al., 2016). The short-term component of $PM_{2.5}$ fluctuated frequently with a significantly positive correlation to the daily change of $PM_{2.5}$ (r = 0.68, p<0.05), indicating an important role of the short-term component with the temporal period < 33 days in the day-to-day variations of $PM_{2.5}$ concentrations in the THB (Fig. 3a).

The notable peaks of $PM_{2.5}$ seasonal components emerged in winters were highly in keeping with the peaks of observed daily $PM_{2.5}$ concentrations (Fig. 3b). A close linkage with the significant correlation coefficient of 0.75 (p<0.05) was found

170   between the changes of $PM_{2.5}$ seasonal components and daily $PM_{2.5}$ concentrations, which could reflect a significant modulation of the $PM_{2.5}$ seasonal oscillations to the day-to-day variations of $PM_{2.5}$, driven by the seasonal shift of East Asian summer and winter monsoons as well as the seasonal change of anthropogenic emissions (Zhu et al., 2012; Jeong and Park, 2017).

The change of long-term component of $PM_{2.5}$ exhibited a steadily declining trend over 2015-2019 (Fig. 3c), which might

175   be caused by the sustained impact of emission control. The correlation coefficient (r = 0.24, p<0.05) of long-term $PM_{2.5}$ component with the observed daily $PM_{2.5}$ change was much smaller than those of short-term and seasonal $PM_{2.5}$ components, implying less influence of emission reduction on the daily $PM_{2.5}$ change and air pollution frequency, although the declining trend in $PM_{2.5}$ was determined by anthropogenic emission reduction.

180   **3.2 Multiple linear regressions of $PM_{2.5}$, SO_2 and NO_2 with meteorological drivers**

Since the short-term variations in meteorological variables were excluded, the correlations between baseline components of $PM_{2.5}$ and meteorological variables were only related to their seasonal and long-term components, affected by regional climate of East Asian monsoons rather than synoptic-scale meteorological processes. Generally, the baseline components of

air pollutants were negatively correlated with baseline components of wind speed (WS_{BL}) and positively correlated with

185 baseline components of sea level pressure (SLP_{BL}) (Table S1–S3), which could be attributed to the ventilation effect of wind

and stagnant condition of meteorology in high-pressure systems, restraining the horizontal and vertical dispersions of air

pollutants (Hsu and Cheng, 2016; Wang et al., 2016; Miao et al., 2017). Although wind speed exerts a negative influence of

on $PM_{2.5}$ concentrations over the emission source region, increasing wind speed might cause the accumulation of $PM_{2.5}$

concentrations over the downwind region of emission sources (Chen et al., 2020), which led to the inconsistent influence of

190 WS_{BL} in the region of central China (Table S1–S3). Under surface high air temperature conditions, there are strong thermal

activities such as turbulence, making an accelerated dispersion of air pollutants (Yang et al., 2016b). The negative influence of

RH_{BL} and T_{BL} on $PM_{2.5BL}$, SO_{2BL} and NO_{2BL} mainly reflected the effect of seasonal cycle in East Asian winter and summer

monsoons, whereas the influence of precipitation on air pollutants was more straightforward than other meteorological

parameters, negatively influencing surface pollutant concentrations through the precipitation washout of air pollutants (Table

195 S1–S3).

To isolate emission-related long-term components from long-term components of $PM_{2.5}$, NO_2 and SO_2, the stepwise

multiple linear regressions of $PM_{2.5BL}$, SO_{2BL} and NO_{2BL} respectively with baseline components of meteorological parameters

(T_{BL}, WS_{BL}, RH_{BL}, SLP_{BL} and Pre_{BL}) were conducted with Eq. (7) in 14 sites, by adding and deleting meteorological variables

based on the independent statistical significance to obtain the best model fit (Draper, 1998). We evaluated the $PM_{2.5BL}$, SO_{2BL}

200 and NO_{2BL} fitted by the multiple linear regression models with the KZ decomposition (Table 1). The multiple linear regressions

explained $PM_{2.5BL}$, SO_{2BL} and NO_{2BL} with adjusted determination coefficients (Adj. R^2) of 0.5695–0.8093, 0.0630–0.4592 and

0.6304–0.8669 passing the confidence level of 99% in all the THB sites. The Adj. R^2 of multiple linear regression for SO_{2BL}

were lower than those of $PM_{2.5BL}$ and NO_{2BL}, which might be attributed to the larger impact of SO_2 emission control on the

seasonal and long-term SO_2 variations. In general, the variations of meteorological drivers can well reproduce the meteorology-

205 related seasonal and long-term variations of $PM_{2.5}$, SO_2 and NO_2 in the THB (Table 1).

3.3 Interannual variations in air pollutants observed over the THB

PM$_{2.5}$ consists of chemical components generated in the complex physical and chemical processes (Li et al., 2015a). Primary particles are emitted directly from anthropogenic (e.g., industry, power plants, and vehicles) and natural (e.g., outdoor

210   biomass burning and dust storms) sources. Secondary particles(e.g. sulfate and nitrate) are converted with chemical reactions of the precursor gases (e.g., SO$_2$ and NOx) , which are mainly produced by human activities (Li et al., 2015a; Yang et al., 2016a). Therefore, in addition to the reductions in primary particulate emissions, control of the secondary aerosol precursor emissions is of great importance in mitigating air pollution.

The interannual variations of the ratios in annual mean PM$_{2.5}$, SO$_2$ and NO$_2$ concentrations relative to the annual averages

215   in 2015 over the THB are displayed in Figure 4. The declines of PM$_{2.5}$ and SO$_2$ in 2019 averaged over the THB were -26% and -68% relative to 2015, while the decrease ratio in NO$_2$ was only -8% over this region. The observed SO$_2$ concentrations had a steeper decrease than PM$_{2.5}$ and NO$_2$, possibly because the dominant source sectors (i.e., power and industry) of SO$_2$ significantly reduced their emissions (Zheng et al., 2018). The power sector was the major contributor to emission reduction but only accounted for one-third of NO$_X$ emissions and the contribution of transportation to NO$_X$ emissions was estimated to

220   have increased over recent years (Zheng et al., 2018).

Figure 5 shows the spatial distributions of 5-year averaged concentrations, the linear trends and the change rates in interannual variations of PM$_{2.5}$, SO$_2$ and NO$_2$ observed in the THB over 2015–2019. The change rates (% yr^{-1}) were calculated with the linear trends by dividing with temporal-mean concentrations of air pollutants at the observation sites for the analysis period in Figure 5. The 5-year averaged PM$_{2.5}$ concentrations over the THB exceeded the Chinese National secondary air

225   quality standard of 35 μg m^{-3} for annual mean PM$_{2.5}$ concentration (Fig. 5a), while SO$_2$ and NO$_2$ concentrations reached the secondary standards of 60 μg m^{-3} and 40 μg m^{-3} in annual mean SO$_2$ and NO$_2$ concentrations at most sites over the THB (Figs. 5d and 5g). Specifically, the 5-year averaged NO$_2$ concentrations exceeded 40 μg m^{-3} in WH (Wuhan), the mega-city in central China, that might be attributable to the large amounts of traffic transportation. From 2015 to 2019, both PM$_{2.5}$ and SO$_2$ decreased at all sites over the THB (Figs. 5b and 5e), whereas NO$_2$ trends were changed from mostly negative to positive in

230   some sites (Fig. 5h), possibly due to the spatial disparity of NOx emissions in traffic sectors (Zheng et al., 2018). The

comparison among the change rates of $PM_{2.5}$, SO_2 and NO_2 in the THB presented the largest decreases of SO_2 with -20% – -

40% yr^{-1} over the five years (Figs. 5c, 5f and 5i), reflecting the effective control of SO_2 emissions in terms of primary gaseous

pollutants.

There were obvious decreases in regional mean $PM_{2.5}$, SO_2 and NO_2 concentrations over the THB (Fig. 4), while the

235   declining degree of $PM_{2.5}$ and SO_2 varied from site to site over the THB and the change trends in NO_2 were weak negative and

even positive in certain sites (Figs. 5c, 5f and 5i). These interannual changes of air pollutants in the THB over recent years

were investigated with the emission- and meteorology-related long-term components of air pollutants in the next sections.

3.4 Effects of NO_2 and SO_2 emission reductions on $PM_{2.5}$ change trends

240   The declining trend of $PM_{2.5}$ in China could be partly attributed to the reduced NO_x and SO_2 concentrations for producing

the secondary aerosols (Zhang et al., 2018). The reduction rates of anthropogenic emissions have markedly accelerated after

2013, decreasing by 59% for SO_2, 21% for NOx and 33% for $PM_{2.5}$ during 2013–2017 over the THB region (Zheng et al.,

2018). In order to assess the effect of changing precursor pollutant emissions on $PM_{2.5}$ declines, we compared the linear trends

of emission-related long-term components of $PM_{2.5}$, NO_2 and SO_2 decomposed based on Eq. (9) over the THB for 2015–2019

245   (Fig. 6). The distinct declining trends of emission-related long-term $PM_{2.5}$ and SO_2 components as well as the variable trends

of emission-related long-term NO_2 components were distributed basically consistent with the positive and negative trends in

the interannual variations of air pollutant concentrations in the THB (Fig.5 (middle column); Fig. 6), demonstrating that the

local emissions of air pollutants could spatially dominate the long-term variations of air pollutants in central China, especially

the increasing trends in NO_2 at some THB sites.

250    $PM_{2.5}$ concentrations are changed by emissions of both primary $PM_{2.5}$ and $PM_{2.5}$'s gaseous precursors. As major gaseous

precursors, SO_2 and NO_2 can be oxidized to convert nitrate and sulfate for secondary $PM_{2.5}$ (Li et al., 2015a). To investigate

the effects of emission reductions on the interannual variations of $PM_{2.5}$, NO_2 and SO_2 over recent years, the ratios of change

trends in long-term (k_{LT}) and emission-related long-term (k_{emiss}) components of $PM_{2.5}$, SO_2 and NO_2, in the THB over 2015–

2019 were demonstrated in Figure 7, where the long-term and emission-related long-term components of $PM_{2.5}$, SO_2 and NO_2

255 were calculated with Eqs. (4) and (9). The trend ratios k_{LT}/k_{emiss} <1 indicated the more obvious downward trend of emission-

related long-term variations than the long-term trend of air pollutant concentrations, which might be attributed to the offsetting

effect of meteorological conditions on emission reduction in air quality change, whereas the long-term trend of air pollutant

concentrations was more significant than the emission-related long-term trend with k_{LT}/k_{emiss} >1, reflecting the synchronous

impacts of anthropogenic emissions and meteorology on the long-term trend in air pollutant change. In addition, the trend

260 ratios k_{LT}/k_{emiss} >1 and k_{LT}/k_{emiss} <1 of $PM_{2.5}$'s gaseous precursors SO_2 and NO_2 could reflect the high and weak

efficiencies of SO_2 and NO_2 converting to sulfate and nitrate in the production of secondary $PM_{2.5}$ during air pollutant emission

reduction. The notable differences in Figure 7 were spatially distributed with the trend ratios k_{LT}/k_{emiss} >1 and k_{LT}/k_{emiss}

<1 in $PM_{2.5}$, SO_2 and NO_2 concentrations under the same meteorological conditions, indicating the different influences of

emissions on the long-term variations of $PM_{2.5}$, SO_2 and NO_2 in the THB during recent years. The reduction in $PM_{2.5}$ emissions

265 was a primary cause for the long-term declines in $PM_{2.5}$ concentrations in the THB, even though the meteorological changes

might offset the effects of emission reduction on air quality improvement over the southern THB (Figs. 6 and 7). It is

noteworthy that the trend ratios k_{LT}/k_{emiss} <1 of $PM_{2.5}$ were accompanied with k_{LT}/k_{emiss} >1 of SO_2 and NO_2 at the

downwind southern THB sites with both negative k_{LT} and k_{emiss} (Fig. 7, Table S4), which could imply the increasing

conversion efficiency of SO_2 and NO_2 to sulfate and nitrate for secondary $PM_{2.5}$ during the reductions of air pollutant emissions

270 over recent years. In the upwind northern THB sites, the k_{LT}/k_{emiss} >1 of $PM_{2.5}$ were accompanied with k_{LT}/k_{emiss} >1

of SO_2 and NO_2 with obviously facilitating effect of meteorology on $PM_{2.5}$ decline (Fig. 7, Table S4), revealing the

underlying effect of regional transport of air pollutants on the spatial distribution of conversion efficiency of gaseous precursor

to secondary $PM_{2.5}$.

    In order to further assess the effect of gaseous precursor emissions on $PM_{2.5}$ declines during recent 5-year air pollution

275 mitigation, we selected 7 and 9 sites in the THB with the decreasing trends of emission-related long-term SO_2 and NO_2

components below -0.5 and 0.0 µg m^{-3} 100d^{-1} respectively (Table S4) to compare the trend ratios $k_{\mathrm{LT}}/k_{emiss}$ of PM$_{2.5}$, NO$_2$

and SO$_2$ for 2015–2019 (Fig. 8). The significantly negative linear correlations between changes in $k_{\mathrm{LT}}/k_{emiss}$ of gaseous

precursors (SO$_2$ and NO$_2$) and PM$_{2.5}$ could present the connection of $k_{\mathrm{LT}}/k_{emiss}$ > 1 for NO$_2$ and SO$_2$ with $k_{\mathrm{LT}}/k_{emiss}$ < 1

for PM$_{2.5}$, which confirmed the fact that the high conversion efficiency of SO$_2$ and NO$_2$ to sulfate and nitrate could offset the

280 role of PM$_{2.5}$ emission reduction in controlling PM$_{2.5}$ pollution. This study identified the enhancing contribution of gaseous

precursor emissions to PM$_{2.5}$ concentrations with reducing anthropogenic emissions of air pollutants over the receptor region

in regional PM$_{2.5}$ transport.

3.5 Meteorological contribution to PM$_{2.5}$ change trends

285 As the air pollutant change trend is assumed to generally consist of emission- and meteorology-related changes (Seo et

al., 2018; Yin et al., 2019b), the meteorological contribution rate Con_{met} to long-term PM$_{2.5}$ change trend is calculated with

the following equation:

$$Con_{met} = \frac{k_{\mathrm{LT}} - k_{emiss}}{k_{LT}} \times 100\%. \tag{10}$$

Here, Con_{met} (in %) is estimated with the linear trends k_{LT} of long-term component $PM_{2.5LT}(t)$ and k_{emiss} of emission-

290 related long-term component $PM_{2.5LT}^{emiss}(t)$. $PM_{2.5LT}(t)$ and $PM_{2.5LT}^{emiss}(t)$ are respectively calculated with Eqs. (4) and (9).

To quantitatively assess the meteorological contributions to the PM$_{2.5}$ declining trends, the linear trends k_{LT} and k_{emiss}

with the meteorological contribution rate Con_{met} in Eq. (10) were presented in Table S5 for 14 sites over the THB during

2015-2019. All the trends k_{LT} and k_{emiss} respectively in $PM_{2.5LT}(t)$ and $PM_{2.5LT}^{emiss}(t)$ were negative over the THB

(Table S5), indicating the significant effect of emission reductions on PM$_{2.5}$ declining trends for improving regional air quality

295 in central China. By comparing the PM$_{2.5}$ declining trends k_{emiss} and k_{LT} from site to site (Table S5), the positive and

negative contributions of meteorological variations to PM$_{2.5}$ change trends over recent years were determined with the positive

and negative differences between k_{emiss} and k_{LT} with the distinct meteorological influences on the change of THB's

regional environment.

The spatial distribution of meteorological contribution rates Con_{met} to long-term PM$_{2.5}$ declining trend presented the

300   unique pattern of northern positive and southern negative values over the THB (Fig. 9), with the high positive contributions in

northern sites XY (61.92%) and EZ (37.31%) as well as low negative contributions in southern sites CD (-24.93%) and CS (-

23.03%). Comparing with the statistical studies of meteorological influence on regional PM$_{2.5}$ changes in other regions over

China with the meteorological contribution of about 20% over recent years (Chen et al., 2019; Zhai et al., 2019), the PM$_{2.5}$

pollution over the THB was affected contrarily by meteorological drivers with the northern positive and southern negative

305   contribution from 2015 to 2019 (Fig. 9). The meteorological change could accelerate and offset the effects of emission

reductions on PM$_{2.5}$ declining trends in the northern and southern THB, which might be attributed to regional transport of air

pollutants conducive to the upwind diffusion and downward accumulation of air pollutants respectively over the northern and

southern THB under the declining wind of East Asian monsoons over recent years (Hu et al., 2020; Zhong et al., 2019).

310   **4.   Conclusions**

The observational data of environment and meteorology from 2015 to 2019 were achieved to investigate the characteristics

and causes of PM$_{2.5}$ reductions in the THB, a receptor region in regional transport of air pollutants in central China. This study

decomposed the observed PM$_{2.5}$ concentrations into multi-time scale components with a modified KZ filter, to better

understand the PM$_{2.5}$ variations with the short-term, seasonal and long-term components accounting for respectively 47.5%,

315   41.4% and 3.7% to observed PM$_{2.5}$ changes. The short-term and seasonal PM$_{2.5}$ components dominated the daily PM$_{2.5}$ changes

and long-term component determined the trend of PM$_{2.5}$ change over recent years. The long-term components of PM$_{2.5}$, SO$_2$

and NO$_2$ were further isolated into emission- and meteorology-related long-term components with multiple linear regressions,

to figure out the contributions of emission and meteorology to PM$_{2.5}$ decline in the THB over 2015–2019. The reduction in

anthropogenic emissions was the primary cause for long-term decline in PM$_{2.5}$ concentrations and the meteorological changes

320   moderated the PM$_{2.5}$ variations in the THB. As the receptor region of regional PM$_{2.5}$ transport, the impact of diverse

meteorological conditions on long-term trend of PM$_{2.5}$ changes displayed unique regional pattern of northern positive rates up

to 61.92% and southern negative rates down to -24.93%. The change of meteorological conditions could accelerate and offset

the effects of emission reductions on $PM_{2.5}$ declining trends in the northern and southern THB, which could be attributed to

the upwind diffusing and downward accumulating roles of regional transport pathway on air pollutants in the THB. In terms

325   of gaseous precursor emissions, the increasing conversion efficiency of SO_2 and NO_2 to sulfate and nitrate for secondary $PM_{2.5}$

could offset the role of $PM_{2.5}$ emission reduction in controlling air pollution, and the contribution of gaseous precursor

emissions to secondary $PM_{2.5}$ enhanced with the reducing anthropogenic emissions of air pollutants over this receptor region.

This study exposed the impact of anthropogenic emissions and meteorological conditions on the $PM_{2.5}$ decline over a

receptor region in regional transport of air pollutants in central China. The effect of regional transport on $PM_{2.5}$ pollution over

330   the receptor region was found differing from that over the source regions with high anthropogenic emissions. To generalize

our finding, further work could be desired with climate analyses of long-term observations of air pollutants and more

comprehensively modeling of air quality and meteorology.

Data availability. Data used in this paper can be provided upon request from Xiaoyun Sun (sunxy6362@126.com) or Tianliang

335   Zhao (tlzhao@nuist.edu.cn).

Author contributions. TZ and XS conceived the study. YB provided the observation data. XS designed the graphics and wrote

the manuscript with help from TZ and SK. HZ, WH, XM and JX were involved in the scientific discussion. All authors

commented on the paper.

340

Competing interests. The authors declare that they have no conflict of interest.

Acknowledgement. This research was financially funded by grants from National Natural Science Foundation of China

(41830965; 42075186; 91744209) and the National Key R & D Program Pilot Projects of China (2016YFC0203304).

345

References

Cao, J. J., Wang, Q. Y., Chow, J. C., Watson, J. G., Tie, X. X., Shen, Z. X., Wang, P., and An, Z. S.: Impacts of aerosol compositions on visibility impairment in Xi'an, China, Atmospheric Environment, 59, 559-566, 2012.

Chen, Z. Y., Chen, D. L., Kwan, M. P., Chen, B., Gao, B. B., Zhuang, Y., Li, R. Y., and Xu, B.: The control of anthropogenic emissions contributed to 80 % of the decrease in PM 2.5 concentrations in Beijing from 2013 to 2017, Atmospheric Chemistry and Physics, 19, 13519-13533, 2019.

Chen, Z. Y., Chen, D. L., Zhao, C. F., Kwan, M.-P., Cai, J., Zhuang, Y., Zhao, B., Wang, X. Y., Chen, B., and Yang, J.: Influence of meteorological conditions on PM2. 5 concentrations across China: A review of methodology and mechanism, Environment International, 139, 105558, 2020.

Crouse, D. L., Peters, P. A., van Donkelaar, A., Goldberg, M. S., Villeneuve, P. J., Brion, O., Khan, S., Atari, D. O., Jerrett, M., and Pope III, C. A.: Risk of nonaccidental and cardiovascular mortality in relation to long-term exposure to low concentrations of fine particulate matter: a Canadian national-level cohort study, Environmental Health Perspectives, 120, 708-714, 2012.

Draper, N. R.: Applied regression analysis, Technometrics, 9, 182-183, 1998.

Eskridge, R. E., Ku, J. Y., Rao, S. T., Porter, P. S., and Zurbenko, I. G.: Separating different scales of motion in time series of meteorological variables, Bulletin of the American Meteorological Society, 78, 1473-1484, 1997.

Gong, S. L., Liu, H. L., Zhang, B. H., He, J. J., Zhang, H. D., Wang, Y. Q., Wang, S. X., Zhang, L., and Wang, J.: Assessment of meteorology vs. control measures in the China fine particular matter trend from 2013 to 2019 by an environmental meteorology index, Atmospheric Chemistry and Physics, 21, 2999-3013, 10.5194/acp-21-2999-2021, 2021.

Gui, K., Che, H. Z., Wang, Y. Q., Wang, H., Zhang, L., Zhao, H. J., Zheng, Y., Sun, T. Z., and Zhang, X. Y.: Satellite-derived PM2. 5 concentration trends over Eastern China from 1998 to 2016: Relationships to emissions and meteorological parameters, Environmental Pollution, 247, 1125-1133, 2019.

Guo, H., Cheng, T. H., Gu, X. F., Wang, Y., Chen, H., Bao, F. W., Shi, S. Y., Xu, B. R., Wang, W. N., Zuo, X., Zhang, X. C.,

350

355

360

365

and Meng, C.: Assessment of PM2.5 concentrations and exposure throughout China using ground observations, Sci Total Environ, 601-602, 1024-1030, 10.1016/j.scitotenv.2017.05.263, 2017.

370   Hsu, C.-H., and Cheng, F.-Y.: Classification of weather patterns to study the influence of meteorological characteristics on PM2. 5 concentrations in Yunlin County, Taiwan, Atmospheric Environment, 144, 397-408, 2016.

Hu, W. Y., Zhao, T. L., Bai, Y. Q., Shen, L. J., Sun, X. Y., and Gu, Y.: Contribution of regional PM2. 5 transport to air pollution enhanced by sub-basin topography: A modeling case over central China, Atmosphere, 11, 1258, 2020.

Hu, W. Y., Zhao, T. L., Bai, Y. Q., Kong, S. F., Xiong, J., Sun, X. Y., Yang, Q. J., Gu, Y., and Lu, H. C.: Importance of regional

375   PM2. 5 transport and precipitation washout in heavy air pollution in the Twain-Hu Basin over Central China: Observational analysis and WRF-Chem simulation, Science of the Total Environment, 758, 143710, 2021.

Jeong, J. I., and Park, R. J.: Winter monsoon variability and its impact on aerosol concentrations in East Asia, Environ Pollut, 221, 285-292, 10.1016/j.envpol.2016.11.075, 2017.

Kim, Y. M., Seo, J. H., Kim, J. Y., Lee, J. Y., Kim, H. J., and Kim, B. M.: Characterization of PM 2.5 and identification of

380   transported secondary and biomass burning contribution in Seoul, Korea, Environmental Science and Pollution Research, 25, 4330-4343, 2018.

Li, G. H., Zavala, M., Lei, W., Tsimpidi, A. P., Karydis, V. A., Pandis, S. N., Canagaratna, M. R., and Molina, L. T.: Simulations of organic aerosol concentrations in Mexico City using the WRF-CHEM model during the MCMA-2006/MILAGRO campaign, Atmospheric Chemistry and Physics, 11, 3789-3809, 2011.

385   Li, K., Liao, H., Cai, W. J., and Yang, Y.: Attribution of anthropogenic influence on atmospheric patterns conducive to recent most severe haze over eastern China, Geophysical Research Letters, 45, 2072-2081, 2018.

Li, S., Ren, A. L., Guo, B., Du, Z., Zhang, S., Tian, M., and Wang, S. S.: Influence of Meteorological Factors and VOCs on PM2. 5during Severe Air Pollution Period in Shijiazhuang in Winter, 2015 2nd International Conference on Machinery, Materials Engineering, Chemical Engineering and Biotechnology, 2015a, 588-592.

390   Li, X., Zhang, Q., Zhang, Y., Zheng, B., Wang, K., Chen, Y., Wallington, T. J., Han, W. J., Shen, W., and Zhang, X. Y.: Source

contributions of urban PM2. 5 in the Beijing–Tianjin–Hebei region: Changes between 2006 and 2013 and relative impacts of

emissions and meteorology, Atmospheric Environment, 123, 229-239, 2015b.

Lin, C. Q., Liu, G. H., Lau, A. K. H., Li, Y., Li, C. C., Fung, J. C. H., and Lao, X. Q.: High-resolution satellite remote sensing

of provincial PM2. 5 trends in China from 2001 to 2015, Atmospheric Environment, 180, 110-116, 2018.

395   Lu, M. M., Tang, X., Wang, Z. F., Gbaguidi, A., Liang, S. W., Hu, K., Wu, L., Wu, H. J., Huang, Z., and Shen, L. J.: Source

tagging modeling study of heavy haze episodes under complex regional transport processes over Wuhan megacity, Central

China, Environmental Pollution, 231, 612-621, 2017.

Ma, Z. Q., Xu, J., Quan, W. J., Zhang, Z. Y., Lin, W. L., and Xu, X. B.: Significant increase of surface ozone at a rural site,

north of eastern China, Atmospheric Chemistry and Physics, 16, 3969-3977, 2016.

400   Miao, Y. C., Hu, X. M., Liu, S. H., Qian, T. T., Xue, M., Zheng, Y. J., and Wang, S.: Seasonal variation of local atmospheric

circulations and boundary layer structure in the Beijing-Tianjin-Hebei region and implications for air quality, Journal of

Advances in Modeling Earth Systems, 7, 1602-1626, 2015.

Miao, Y. C., Guo, J. P., Liu, S. H., Liu, H., Li, Z. Q., Zhang, W. C., and Zhai, P. M.: Classification of summertime synoptic

patterns in Beijing and their associations with boundary layer structure affecting aerosol pollution, Atmospheric Chemistry

405   and Physics, 17, 3097-3110, 2017.

Mueller, S. F., and Mallard, J. W.: Contributions of natural emissions to ozone and PM2. 5 as simulated by the community

multiscale air quality (CMAQ) model, Environmental science & technology, 45, 4817-4823, 2011.

Ning, G. C., Yim, S. H. L., Wang, S. G., Duan, B. L., Nie, C. Q., Yang, X., Wang, J. Y., and Shang, K. Z.: Synergistic effects

of synoptic weather patterns and topography on air quality: a case of the Sichuan Basin of China, Climate Dynamics, 53, 6729-

410   6744, 2019.

Pearce, J. L., Beringer, J., Nicholls, N., Hyndman, R. J., and Tapper, N. J.: Quantifying the influence of local meteorology on

air quality using generalized additive models, Atmospheric Environment, 45, 1328-1336, 2011.

Peng, J., Chen, S., Lü, H. L., Liu, Y. X., and Wu, J. S.: Spatiotemporal patterns of remotely sensed PM2. 5 concentration in

China from 1999 to 2011, Remote Sensing of Environment, 174, 109-121, 2016.

415 Rao, S. T., and Zurbenko, I. G.: Detecting and tracking changes in ozone air quality, Air & waste, 44, 1089-1092, 1994.

Russell, A. R., Valin, L. C., Bucsela, E. J., Wenig, M. O., and Cohen, R. C.: Space-based constraints on spatial and temporal

patterns of NO x emissions in California, 2005− 2008, Environmental science & technology, 44, 3608-3615, 2010.

Seo, J., Youn, D., Kim, J. Y., and Lee, H.: Extensive spatiotemporal analyses of surface ozone and related meteorological

variables in South Korea for the period 1999–2010, Atmospheric Chemistry and Physics, 14, 6395-6415, 2014.

420 Seo, J., Kim, J. Y., Youn, D., Lee, J. Y., Kim, H., Lim, Y. B., Kim, Y., and Jin, H. C.: On the multiday haze in the Asian

continental outflow: the important role of synoptic conditions combined with regional and local sources, Atmospheric

Chemistry and Physics, 17, 9311-9332, 2017.

Seo, J., Park, D. S. R., Kim, J. Y., Youn, D., Lim, Y. B., and Kim, Y.: Effects of meteorology and emissions on urban air quality:

a quantitative statistical approach to long-term records (1999–2016) in Seoul, South Korea, Atmospheric Chemistry and

425 Physics, 18, 16121-16137, 2018.

Shen, L. J., Wang, H. L., Zhao, T. L., Liu, J., Bai, Y. Q., Kong, S. F., and Shu, Z. Z.: Characterizing regional aerosol pollution

in central China based on 19 years of MODIS data: Spatiotemporal variation and aerosol type discrimination, Environmental

Pollution, 263, 114556, 10.1016/j.envpol.2020.114556, 2020.

Sun, Y., Song, T., Tang, G. Q., and Wang, Y. S.: The vertical distribution of PM2. 5 and boundary-layer structure during summer

430 haze in Beijing, Atmospheric Environment, 74, 413-421, 2013.

Tang, G. Q., Zhang, J. Q., Zhu, X. W., Song, T., Münkel, C., Hu, B., Schäfer, K., Liu, Z. R., Zhang, J. K., and Wang, L. L.:

Mixing layer height and its implications for air pollution over Beijing, China, Atmospheric Chemistry and Physics, 16, 2459-

2475, 2016.

Wang, X. Y., Wang, K. C., and Su, L. Y.: Contribution of atmospheric diffusion conditions to the recent improvement in air

435 quality in China, Scientific reports, 6, 1-11, 2016.

Xue, T., Liu, J., Zhang, Q., Geng, G. N., Zheng, Y. X., Tong, D., Liu, Z., Guan, D. B., Bo, Y., and Zhu, T.: Rapid improvement

of PM 2.5 pollution and associated health benefits in China during 2013–2017, Science China Earth Sciences, 62, 1847-1856, 2019.

Yang, H., Chen, J., Wen, J., Tian, H., and Liu, X.: Composition and sources of PM2.5 around the heating periods of 2013 and

440   2014 in Beijing: Implications for efficient mitigation measures, Atmospheric Environment, 124, 378-386, 10.1016/j.atmosenv.2015.05.015, 2016a.

Yang, Y., Liao, H., and Lou, S.: Increase in winter haze over eastern China in recent decades: Roles of variations in meteorological parameters and anthropogenic emissions, Journal of Geophysical Research: Atmospheres, 121, 13,050-013,065, 10.1002/2016jd025136, 2016b.

445   Yin, C. Q., Deng, X. J., Zou, Y., Solmon, F., Li, F., and Deng, T.: Trend analysis of surface ozone at suburban Guangzhou, China, Sci Total Environ, 695, 133880, 10.1016/j.scitotenv.2019.133880, 2019a.

Yin, C. Q., Deng, X. J., Zou, Y., Solmon, F., Li, F., and Deng, T.: Trend analysis of surface ozone at suburban Guangzhou, China, Science of The Total Environment, 695, 133880, 2019b.

Yu, C., Zhao, T. L., Bai, Y. Q., Zhang, L., Kong, S. F., Yu, X. N., He, J. H., Cui, C. G., Yang, J., and You, Y. C.: Heavy air

450   pollution with a unique "non-stagnant" atmospheric boundary layer in the Yangtze River middle basin aggravated by regional transport of PM 2.5 over China, Atmospheric Chemistry and Physics, 20, 7217-7230, 2020.

Zhai, S., Jacob, D. J., Wang, X., Shen, L., Li, K., Zhang, Y., Gui, K., Zhao, T., and Liao, H.: Fine particulate matter (PM2.5) trends in China, 2013–2018: separating contributions from anthropogenic emissions and meteorology, Atmospheric Chemistry and Physics, 19, 11031-11041, 10.5194/acp-19-11031-2019, 2019.

455   Zhang, W. J., Wang, H., Zhang, X. Y., Peng, Y., Zhong, J. T., Wang, Y. Q., and Zhao, Y. F.: Evaluating the contributions of changed meteorological conditions and emission to substantial reductions of PM2. 5 concentration from winter 2016 to 2017 in Central and Eastern China, Science of The Total Environment, 716, 136892, 2020.

Zhang, X. Y., Wang, Y. Q., Niu, T., Zhang, X. C., Gong, S. L., Zhang, Y. M., and Sun, J. Y.: Atmospheric aerosol compositions in China: spatial/temporal variability, chemical signature, regional haze distribution and comparisons with global aerosols,

460   Atmospheric Chemistry and Physics, 12, 779-799, 2012.

Zhang, X. Y., Xu, X. D., Ding, Y. H., Liu, Y. J., Zhang, H. D., Wang, Y. Q., and Zhong, J. T.: The impact of meteorological

changes from 2013 to 2017 on PM 2.5 mass reduction in key regions in China, Science China Earth Sciences, 62, 1885-1902,

2019.

Zhang, Z. Y., Ma, Z. Q., and Kim, S.-J.: Significant decrease of PM2. 5 in Beijing based on long-term records and Kolmogorov-

465   Zurbenko filter approach, Aerosol and Air Quality Research, 18, 711-718, 2018.

Zheng, B., Tong, D., Li, M., Liu, F., Hong, C. P., Geng, G. N., Li, H. Y., Li, X., Peng, L. Q., and Qi, J.: Trends in China's

anthropogenic emissions since 2010 as the consequence of clean air actions, Atmospheric Chemistry and Physics, 18, 14095-

14111, 2018.

Zheng, H., Kong, S. F., Zheng, M. M., Yan, Y. Y., Yao, L. Q., Zheng, S. R., Yan, Q., Wu, J., Cheng, Y., and Chen, N.: A 5.5-

470   year observations of black carbon aerosol at a megacity in Central China: Levels, sources, and variation trends, Atmospheric

Environment, 232, 117581, 2020.

Zhong, J. T., Zhang, X. Y., Wang, Y. Q., Wang, J. Z., Shen, X. J., Zhang, H. S., Wang, T. J., Xie, Z. Q., Liu, C., and Zhang, H.

D.: The two-way feedback mechanism between unfavorable meteorological conditions and cumulative aerosol pollution in

various haze regions of China, Atmospheric Chemistry and Physics, 19, 3287-3306, 2019.

475   Zhu, J. L., Liao, H., and Li, J. P.: Increases in aerosol concentrations over eastern China due to the decadal-scale weakening

of the East Asian summer monsoon, Geophysical Research Letters, 39, 2012.

Table 1 Adjusted determination coefficients (Adj. R^2) between the baseline components decomposed by KZ filter and fitted

with multiple linear regressions respectively for $PM_{2.5BL}$, SO_{2BL} and NO_{2BL} in 14 sites over the THB. All Adj. R^2 passing the

480   confidence level of 99%.

Sites	Adj. R^2 of multiple linear regressions		
	$PM_{2.5BL}$	SO_{2BL}	NO_{2BL}
JZ	0.6776	0.4166	0.8358
XN	0.6899	0.0630	0.7408
XY	0.7971	0.6741	0.8181
JM	0.7872	0.3612	0.6480
YC	0.7168	0.2980	0.6304
SZ	0.7175	0.3612	0.8669
WH	0.7289	0.2718	0.6653
EZ	0.7162	0.4592	0.7523
HG	0.6937	0.1901	0.7220
HS	0.5695	0.2787	0.6952
CS	0.7307	0.1255	0.7012
YY	0.7501	0.1047	0.7592
XG	0.6755	0.4389	0.7692
CD	0.7017	0.1730	0.6937
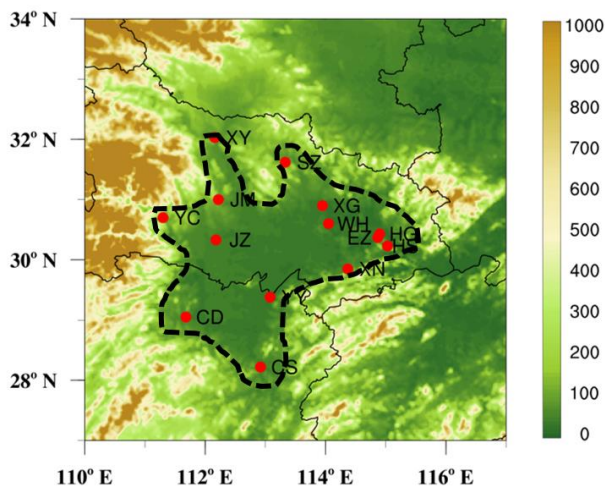
Figure 1 Topographical height (color contours, m, in a. s. l.) over the THB (outlined with black dashed line) with the locations

485   of 14 sites (red dots) and the surrounding regions in central China.
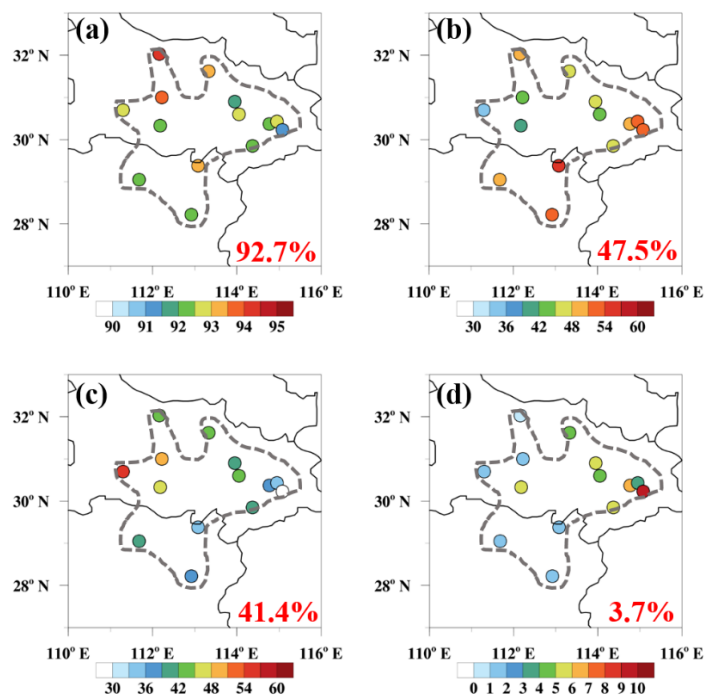
Figure 2 Spatial distributions of the (a) total and relative contributions of (b) short-term, (c) seasonal and (d) long-term

components to the total variances of daily $PM_{2.5}$ changes observed at 14 sites in the THB with the regional averages of 92.7%,

490   47.5%, 41.4% and 3.7%.
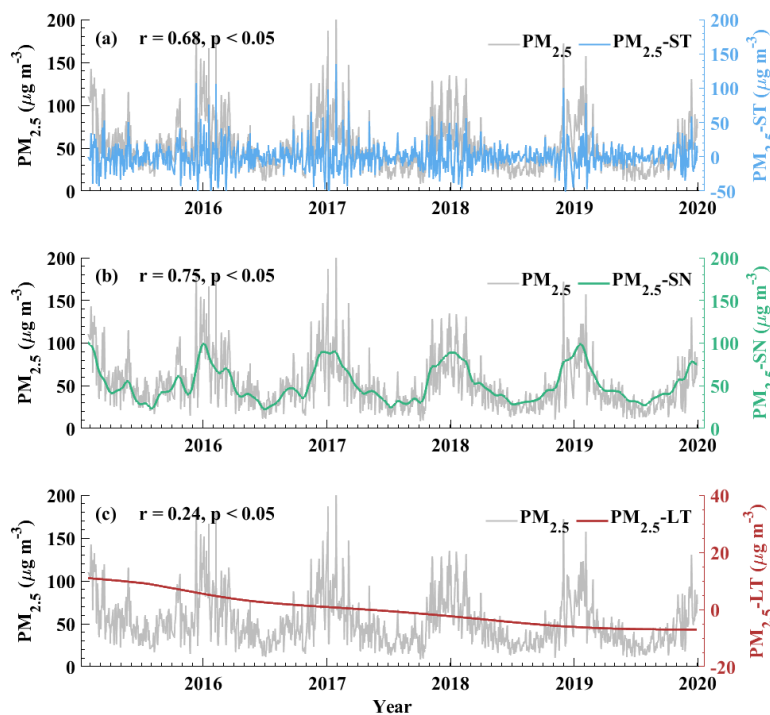
Figure 3 The relations of regional averages of (a) short-term ($PM_{2.5}$-ST), (b) seasonal ($PM_{2.5}$-SN) and (c) long-term ($PM_{2.5}$-LT) components with the observed daily $PM_{2.5}$ concentrations ($PM_{2.5}$) over the THB from 2015 to 2019.

495
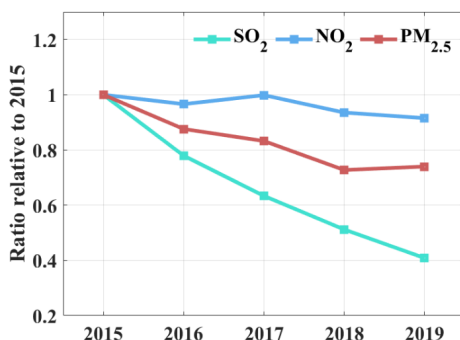
Figure 4 Interannual variations in the ratios of observed annual mean concentrations of SO_2, NO_2 and $PM_{2.5}$ relative to those in 2015 averaged over the THB.
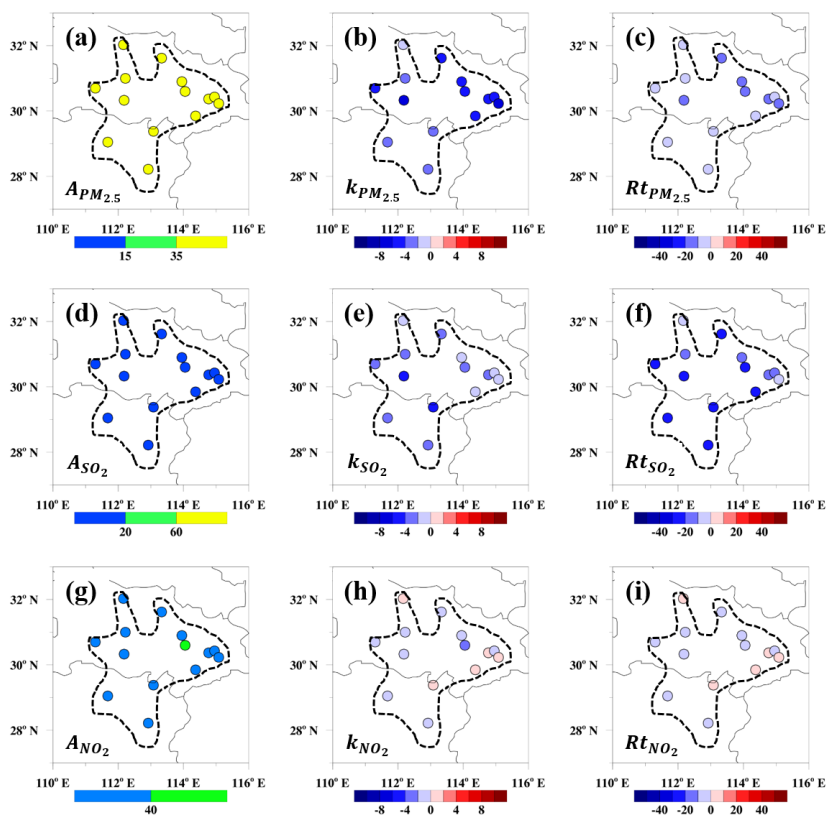
500

Figure 5 Spatial distributions of (left column) 5-year averages of (a) $PM_{2.5}$, (d) SO_2 and (g) NO_2 concentrations (A, unit: μg m⁻

^{3}), (middle column) the linear trends in interannual variations of (b) PM$_{2.5}$, (e) SO$_2$ and (h) NO$_2$ (k, unit: μg m^{-3} yr^{-1}), as well as

(right column) the change rates ($Rt=k/A$, unit: % yr^{-1}) of (c) PM$_{2.5}$, (f) SO$_2$ and (i) NO$_2$ in the THB over 2015–2019.
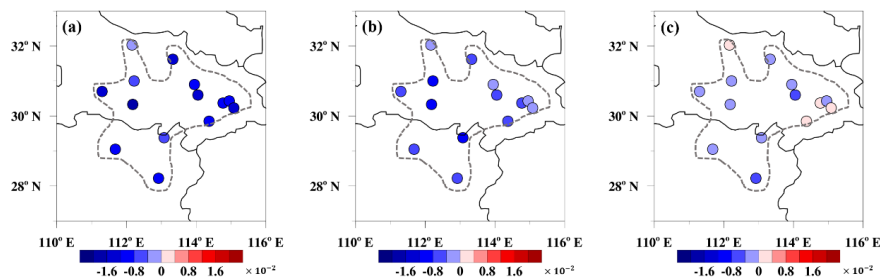
505

Figure 6 Spatial distributions of the linear trends in emission-related long-term components of (a) PM$_{2.5}$, (b) SO$_2$ and (c) NO$_2$

(unit: μg m^{-3} d^{-1}) over 2015–2019 in the THB
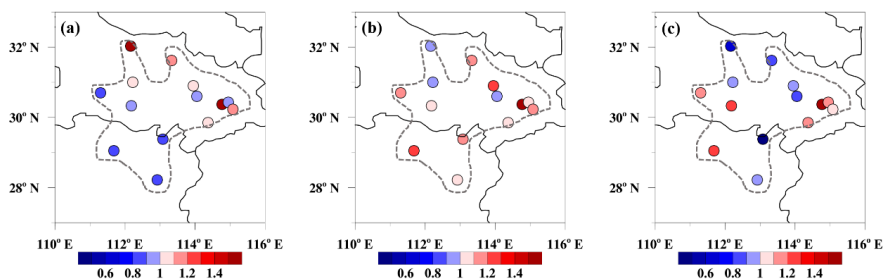
510   **Figure 7** Spatial distributions of the ratios of linear trends in long-term components (k_{LT}) and emission-related long-term

components (k_{emiss}) of (a) PM$_{2.5}$, (b) SO$_2$ and (c) NO$_2$ at 14 sites in the THB over 2015–2019.

10.5194/acp-2021-709
Atmospheric Chemistry and Physics
2021-09-30
journal article
en
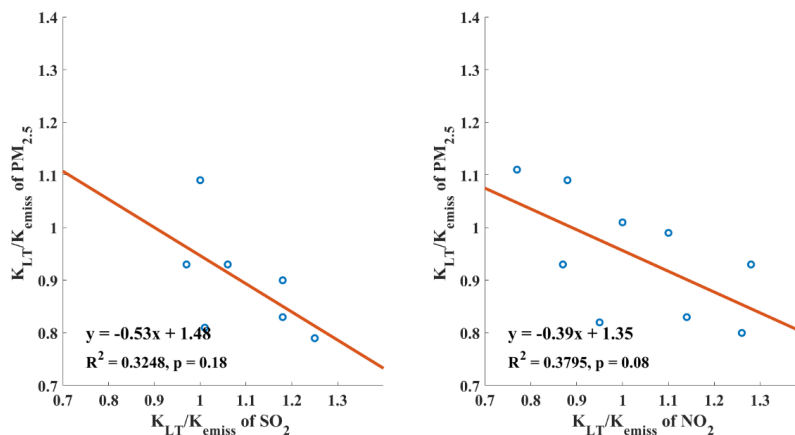
Figure 8 Scatter plots of the ratios between k_{LT} and k_{emiss} of (a) SO₂, (b) NO₂ and PM₂.₅ in the THB from 2015 to 2019

515   with red lines for the linear fitting equations.
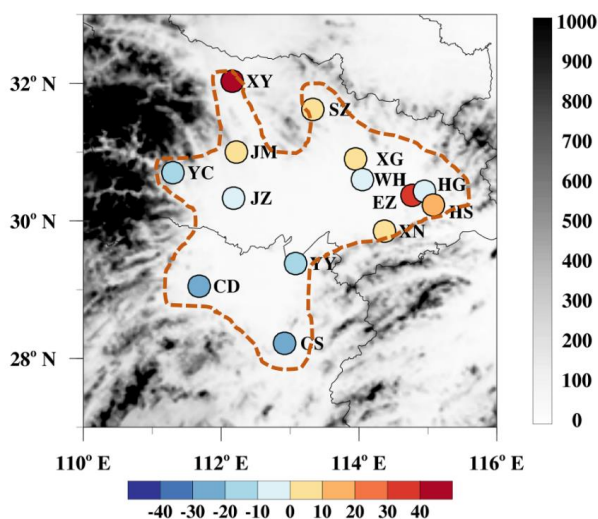
Figure 9 Spatial distribution of contribution rates (colored dots, unit: %) of meteorological variations to PM₂.₅ reductions with

topographical height (color contours, m, in a. s. l.) in the THB (outlined with dashed orange line) and surrounding regions

520   from 2015 to 2019.